ISBN: 978-3-95450-247-9 ISSN: 2673-5490 doi: 10.18429/JACoW-IPAC2024-WEPR25

CONCEPTUAL RF DESIGN AND MODELLING OF A 704 MHz CAVITY FOR THE MUON COOLING COMPLEX*

C. Barbagallo⋆, A. Grudiev, CERN, Geneva, Switzerland

Abstract

The Muon Cooling Complex is a crucial component of the future high-energy Muon Collider, where the ionization cooling technique is employed to reduce muon beam emittance by several orders of magnitude. This cooling technique necessitates the utilization of normal conducting, RF-accelerating cavities operating within a multi-Tesla magnetic field. This study illustrates the conceptual RF design of a 704 MHz copper cavity equipped with beryllium windows for the muon cooling demonstrator. Based on the specifications from the beam dynamics, frequency-domain eigenmode simulations have been conducted to calculate the primary RF figure of merits for the cavity. Subsequently, the cavity geometry has been optimized based on the results obtained from the eigenmode simulations. In a selected case, more advanced engineering analyses, including thermo-mechanical and Lorentz Force Detuning (LFD) simulations, have been performed to enable operation at gradients of up to 44 MV/m within strong solenoidal magnetic fields of up to 7.2 T.

INTRODUCTION

The muon collider holds promise as an excellent candidate for advancing the frontiers of particle physics [1]. Achieving high luminosity requires high beam brightness. Ionization cooling, a technique to enhance brightness, has been successfully demonstrated by the Muon Ionization Cooling Experiment (MICE) [2]. The International Muon Collider Collaboration (IMCC) has proposed a muon ionization cooling demonstrator to prove the six-dimensional emittance reduction across multiple cooling cells [3]. The preliminary cooling cell design incorporates absorbers to reduce the beam momentum and high-gradient copper (Cu) RF accelerating cavities with thin beryllium (Be) windows to restore its longitudinal momentum. Significant efforts have been dedicated to the design of such RF cavities [4], exemplified by the construction and testing of an 805 MHz cavity with Be windows for a future Muon Collider factory at Fermilab [5].

This paper presents a conceptual RF design of a 704 MHz single-cell Cu cavity with Be windows for a future muon cooling demonstrator. This cavity aims to operate at a high gradient E_{nom} = 44 MV/m within a high peak solenoid field of 7.2 T. The beam dynamics specifications are detailed in [3]. Subsequently, RF eigenmode simulations were conducted using CST® [6] to optimize the cavity shape, focusing on its fundamental mode (FM). RF-thermo-mechanical and LFD simulations were performed in COMSOL® [7] to address the deformation of the cavity shape and the induced frequency shift on the cavity FM.

* work endorsed by the IMCC
⋆ carmelo.barbagallo@cern.ch

RF CAVITY DESIGN

The conceptual 704 MHz single-cell cavity for the muon cooling demonstrator was designed using the elliptical cavity parametrization detailed in [8], as depicted in Fig. 1.

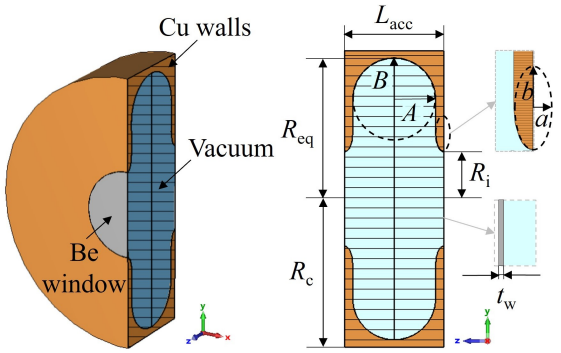

Figure 1: Design of the 704 MHz cavity for muon cooling.

Three geometrical parameters are selected to meet beam dynamics requirements: the accelerating length L_{acc} = 125 mm to achieve an accelerating gradient E_{acc} = 36.44 MV/m for muon beam relativistic factor β = 0.884 (the transient time factor is 0.83); a window with radius R_{i} = 60 mm and thickness t_{w} = 60 µm for adequate beam transmission and to lower the particle scattering. The other parameters are optimized to maximize the shunt impedance $R/Q \cdot Q_0$ (see Table 1) and reduce the surface losses on the window and cavity walls. The peak surface electric field E_{peak} is also minimized to prevent RF-breakdown risk. The geometrical parameters of the optimized geometry are $A = B$ = 52.5 mm, a = 10 mm, b = 22 mm, R_{eq} = 178.71 mm, R_{c} = 188.71mm. The Be windows are integrated to emulate an ideal pillbox, preserving the on-axis E-field and maximizing the shunt impedance. Figures 2 (a) and (b) depict the normalized E-field and H-field maps of the cavity, respectively.

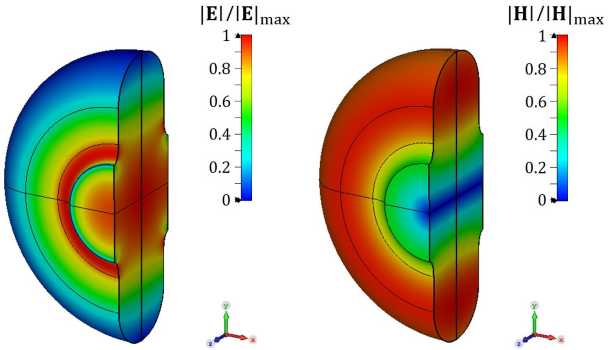

(a) (b)

Figure 2: Normalized E-field (a) and H-field (b) of the cavity.

ISBN: 978-3-95450-247-9 ISSN: 2673-5490 doi: 10.18429/JACoW-IPAC2024-WEPR25

Figure 3 depicts the cavity voltage profile. The filling and decay cavity voltage profiles are provided respectively by:

$$V_{\mathrm{f}} = V_{\mathrm{nom}} \frac{2\beta_{\mathrm{c}}}{1+\beta_{\mathrm{c}}} \left(1 - \mathrm{e}^{-\omega_0 t/2Q_{\mathrm{L}}}\right) \quad \text{and} \quad V_{\mathrm{c}} = V_{\mathrm{nom}} \mathrm{e}^{-\omega_0 t/2Q_{\mathrm{L}}}, \tag{1}$$

where V_{nom} is the cavity's nominal voltage, β_{c} the coupling factor, ω_0 and $Q_{\mathrm{L}} = Q_0/(1+\beta_{\mathrm{c}})$ are the resonant angular frequency and the loaded quality factor of the FM, respectively. The nominal voltage $V_{\mathrm{nom}} = 5.5$ MV is achieved within a filling time of $t_{\mathrm{f}} = 14.46\,\mu$s for $\beta_{\mathrm{c}} = 1.2$ and $Q_{\mathrm{L}} = 1.29\times10^4$. The duration of the injected bunch train at the nominal voltage is $t_{\mathrm{b}} = 0.1\,\mu$s. The beam duty factor (DF) can be calculated as the ratio between the average power and the peak dissipated power:

$$DF = \frac{P_{\mathrm{ave}}}{P_{\mathrm{diss}}} = \frac{\int_0^{\infty} P(t)\mathrm{d}t}{V_{\mathrm{acc}}^2/(R/Q \cdot Q_0)}, \tag{2}$$

where $P(t)$ is the time-dependent power calculated from the cavity voltage profile and V_{acc} the accelerating cavity voltage. Table 1 outlines the relevant RF figures of merit computed for the optimized cavity's FM.

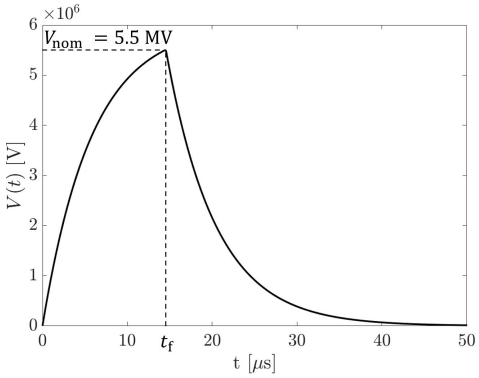

Figure 3: Cavity voltage profile.

Table 1: RF Figures of Merit of the Optimized Cavity

Parameter	Unit	Value	Description
f_0	MHz	704	Operating frequency
Q_0	1	2.83×10^4	Intrinsic quality factor
R/Q	Ω	166.69	Geometric shunt impedance
$R/Q\cdot Q_0$	MΩ	4.72	Shunt impedance
P_{diss}	MW	4.43	Peak dissipated power
DF	1	5.48×10^{-5}	Beam duty factor
P_{ave}	W	242.91	Average power
E_{peak}	MV/m	45.45	Peak surface electric field
B_{peak}	mT	100.03	Peak surface magnetic field

RF-THERMO-MECHANICAL ANALYSES

The second step of our study involves evaluating the dissipated RF power and the steady-state temperature distribution within the cavity and window walls using COMSOL. The dissipated power density on the cavity's inner surfaces due to the FM is implemented as:

$$\frac{\partial P_{\mathrm{ds}}}{\partial A} = \frac{1}{2} R_{\mathrm{s}}(T, f_0)\mathbf{H}_0 \cdot \mathbf{H}_0^*, \tag{3}$$

where $\mathbf{H}_0^*$ denotes the complex conjugate of the magnetic field strength of FM, and $R_{\mathrm{s}}(T, f_0)$ is the temperature-dependent surface resistance at FM frequency [9]. The Dirichlet boundary condition $T = T_0 = 300$ K is employed on the external cavity walls to describe their forced cooling. Figures 4 (a) and (b) illustrate the dissipated power density on the inner surface of the cavity and the window and the resulting temperature distribution in the cavity wall and the window, respectively. The maximum temperature is 312 K, and it is localized at the center of the Be window.

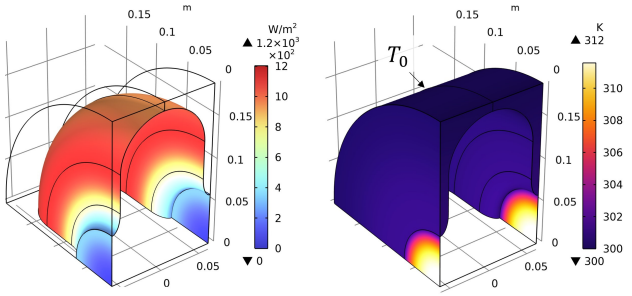

(a) (b)

Figure 4: Dissipated power (a) and maximum temperature (b) on the cavity and window walls.

The obtained temperature distribution serves as input for the non-linear thermo-mechanical simulation. The cavity structure is anchored across its symmetry planes to ensure a unique solution. A moving mesh is utilized in the vacuum-deformed domain, with a roller boundary condition applied on its symmetry planes. The maximum thermally-induced von Mises stress values on the cavity and window walls are 13.40 MPa and 46.10 MPa, respectively. The structure does not undergo thermal plastic deformations since the stress levels are lower than the yield stress of the copper and beryllium, which are 350 MPa and 240 MPa, respectively. Figure 5 depicts the thermally-induced displacement on the cavity mid-plane. The resulting maximum thermally-induced displacement is $u_{\mathrm{th}} = 10.3\,\mu$m, and it is localized on the thin Be window. The thermal strain distribution observed on the window may indicate the occurrence of a buckling effect induced by tangential forces. The thermal deformation shifts the cavity resonance frequency of $\Delta f_{\mathrm{th}} = 14.6$ kHz, which is lower than the cavity bandwidth $\Delta f = 54.69$ kHz.

LORENTZ FORCE DETUNING ANALYSES

The deformation resulting from radiation pressure due to Lorentz forces is studied in the next step of our analysis. The pressure is exerted on the boundary between the cavity and the vacuum domain as [10]:

$$p_{\mathrm{L}} = \frac{1}{4}\left(\mu_0 \mathbf{H}_0^2 - \varepsilon_0 \mathbf{E}_0^2\right), \tag{4}$$

ISBN: 978-3-95450-247-9 ISSN: 2673-5490 doi: 10.18429/JACoW-IPAC2024-WEPR25

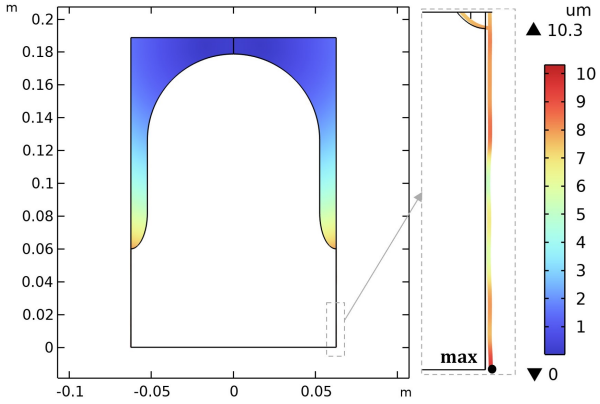

Figure 5: Thermally-induced displacement on the cavity mid-plane (deformed geometry x100).

where $\varepsilon_0 \approx 8.854 \times 10^{-12}$ F/m represents the vacuum permittivity, $\mu_0 \approx 4\pi \times 10^{-7}$ H/m the vacuum permeability, and $\mathbf{E}_0$ and $\mathbf{H}_0$ denote the electric field and magnetic field strengths of FM, respectively. The radiation pressure leads to outward deformation of the cavity walls near the equator and inward deformation near the iris. Figures 6 (a) and (b) depict the radiation pressure map on the cavity and window walls, respectively.

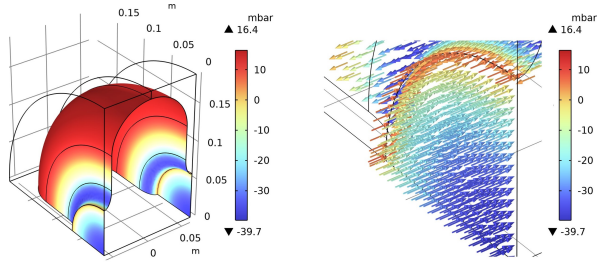

(a) (b)

Figure 6: RF pressure on cavity (a) and window (b) walls.

The maximum inward pressure, which is detected on the window walls, is 45.8 mbar. The maximum von Mises stress is approximately 120 MPa and is localized on the edge connecting the window to the cavity iris. Despite being twice lower than the yield stress of Be, such a high-stress level might still lead to window breaking under mechanical fatigue, posing a risk of contamination to the cavity interior. The resulting maximum displacement induced by radiation pressure is $u_{\mathrm{LFD}} = 936\,\mu\mathrm{m}$, localized at the center of the thin Be window, as depicted in Fig. 7. The mechanical deformation shifts the cavity resonance frequency of $\Delta f_{\mathrm{LFD}} = -0.73$ MHz, which is significantly higher than the cavity bandwidth. The frequency shift is primarily attributed to the significant deformation observed at the window. Furthermore, the simulated window is flat, representing a worst-case scenario. Implementing a curved window could potentially reduce the deformation considerably. Equation (4) is based on the Slater theorem, which is valid only for small deformation. Here, the observed deformation exceeds the thickness of the window by more than a factor of 10. Thus,

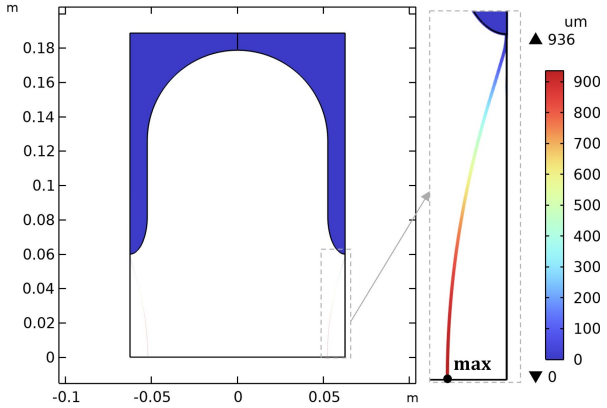

Figure 7: RF pressure-induced displacement on the cavity mid-plane (deformed geometry x10).

Eq. (4) might not accurately represent the applied radiation pressure anymore. Finally, the linear elastic assumption is typically valid within 2-3% of the solid deformations. Even if the model includes geometric non-linearity, the assumption that a purely elastic material can undergo arbitrary large deformations may not be entirely valid.

CONCLUSION

A conceptual RF design and multiphysics models were developed for a Cu 704 MHz cavity with thin Be windows, operating at 44 MV/m, as part of the muon cooling demonstrator. The design was built according to the beam dynamics specifications. The main RF figures of merit and the cavity voltage profile were computed. The majority of the average power is dissipated across the cavity walls. The thermal von Mises stress is lower than the yield stress for both materials. The maximum temperature of 312 K is attained on the cavity window under ideal cooling conditions on the cavity walls. The maximum thermally-induced displacement is 10.3 µm, resulting in a frequency shift of 14.6 kHz, which falls below the cavity bandwidth. A significant RF field pressure is detected on the Be window. The mechanical von Mises stress is lower than the yield stress for both materials. However, the stress level on the Be window is only half the yield stress, posing a potential risk of window rupture under mechanical fatigue. The maximum total displacement induced by Lorentz forces is 936 µm on the Be window, leading to a frequency shift significantly larger than the cavity bandwidth. Considering a new curved window design, like the one in the 805 MHz cavity in [5], may mitigate its deformations and improve its stiffness. An alternative model for simulating LFD in the large deformation regime may also be necessary.

ACKNOWLEDGEMENTS

This work is funded by the European Union (EU). Views and opinions expressed are however those of the author(s) only and do not necessarily reflect those of the EU or European Research Executive Agency (REA). Neither the EU nor the REA can be held responsible for them.

ISBN: 978-3-95450-247-9 ISSN: 2673-5490 doi: 10.18429/JACoW-IPAC2024-WEPR25

REFERENCES

[1] K. Long *et al.*, "Muon colliders to expand frontiers of particle physics", *Nat. Phys.*, vol. 17, no. 3, pp. 289–292, 2021. doi:10.1038/s41567-020-01130-x

[2] MICE collaboration, "Demonstration of cooling by the Muon Ionization Cooling Experiment", *Nature*, vol. 578, no. 7793, pp. 53-59, 2020. doi:10.1038/s41586-020-1958-9

[3] C. Rogers, "A Demonstrator for Muon Ionisation Cooling", *Phys. Sci. Forum*, vol. 8, no. 1, p. 37, 2023. doi:10.3390/psf2023008037

[4] D. Li, A. S. Ladran, D. Lozano, and R. A. Rimmer, "Mechanical and Thermal Analysis of Beryllium Windows for RF Cavities in a Muon Cooling Channel", in *Proc. EPAC'02*, Paris, France, Jun. 2002, paper TUPDO009, pp. 2163–2165.

[5] D. Li *et al.*, "High Power RF Test of an 805 MHz RF Cavity for a Muon Cooling Channel", in *Proc. EPAC'02*, Paris, France, Jun. 2002, paper TUPDO010, pp. 2160–2162.

[6] CST Studio Suite 2023, https://www.cst.com/.

[7] COMSOL Multiphysics 6.2, https://www.comsol.com/.

[8] V. Shemelin, "Optimal choice of cell geometry for a multicell superconducting cavity", *Phys. Rev. Spec. Top. Accel. Beams*, vol. 12, no. 11, p. 114701, 2009. doi:10.1103/PhysRevSTAB.12.114701

[9] H. Guo, B. S. C. Oswald, and P. Arbenz, "Realistic 3-Dimensional Eigenmodal Analysis of Electromagnetic Cavities using Surface Impedance Boundary Conditions", in *Proc. ICAP'12*, Rostock-Warnemunde, Germany, Aug. 2012, paper WEP12, pp. 161–163.

[10] H. Padamsee, J. Knobloch, and T. Hays, *RF Superconductivity for Accelerators*, John Wiley & Sons, 2008.